

Fabrication and Performance Analysis of 4-cm<sup>2</sup> Indium Tin Oxide/InP Photovoltaic Solar Cells\*

T.A. Gessert, X. Li, P.W. Phelps and T.J. Coutts  
Solar Energy Research Institute  
Golden, Colorado

and

N. Tzafaras  
AT&T Microelectronics  
Reading, Pennsylvania

## Introduction

Large-area photovoltaic solar cells based on direct current (dc) magnetron sputter deposition of indium tin oxide (ITO) onto single-crystal p-InP substrates have demonstrated both the radiation hardness and high performance necessary for extraterrestrial applications. (ref. 1) Recently, ITO/InP cells with a total area of 4 cm<sup>2</sup> have been delivered to NASA for flight and experimental analysis on the UoSAT-F satellite, attesting to the advancing maturity of this technology. Although only a small number of these 4-cm<sup>2</sup> ITO/InP cells (approximately 10 cells total) were fabricated for this experiment, the efficiency of the best cell (15.7% at air mass zero [AM0], NASA measurement) compares favorably with the best result reported from a larger production of ~1300 2-cm<sup>2</sup> cells, in which the junction was fabricated through a closed-ampoule diffusion process (16.6% AM0, NASA measurement). (ref. 2)

Because the results mentioned above indicate that the ITO/InP technology is quickly nearing practicality, a small-scale production project has been initiated in which approximately 50 ITO/InP cells are being produced. Through this project, not only is a more representative assessment of the performance of large-area ITO/InP cells being established, but the heretofore assumed advantages of production scale-up are also being tested. This larger volume of cells has also created the opportunity to gain a better understanding of the effect of fabrication procedures on cell performance and has allowed several recently developed process improvements to be further optimized. These improvements include two-gun sputtering, pre-metallization plasma cleaning, and grid/metallization optimization. Performance improvements have been achieved through these changes, resulting in cells with AM0 efficiencies of 16.1% (SERI measurement).

This paper presents and discusses the procedures used in this small-scale production of 4-cm<sup>2</sup> ITO/InP cells. The discussion includes analyses of the performance range of all available production cells, and device performance data of the best cell thus far produced. Additionally, processing experience gained from the production of these cells is discussed, indicating other issues that may be encountered when larger-scale productions are begun.

## Experimental

The materials and processes used for this small-scale production of ITO/InP cells have been developed over many years of research and are discussed in detail elsewhere. (ref. 3 & 4) However, some important process parameters are outlined here. The single-crystal InP substrates were supplied by AT&T Microelectronics (Reading, PA) in two different carrier concentrations of 0.5-2.0 x 10<sup>16</sup> and 1-2 x 10<sup>17</sup> cm<sup>-3</sup> [Zn-doped, (100) orientation]. The substrates were supplied polished on the front side and chemically etched on the back side. Except for cleaning the surfaces in organics, no additional surface preparation was performed before back-contact metallization or ITO deposition (i.e., junction formation). Photoluminescence measurements of these as-received substrates indicated bulk lifetimes very similar to those of other ~2 x 10<sup>16</sup> (Zn-doped) materials used in previous research, demonstrating up to ~10 nsec on unpassivated surfaces.

Prior to junction formation, back-contact metallization was performed using a multistep process involving the vacuum deposition of 120 nm of AuBe (1 weight % Be), annealing, chemical etching, and electrochemical Au plating (1.5 μm). (ref. 5) The ITO deposition was performed in an ULTEK vacuum system using 2-inch planar US Guns in a sputter-up orientation. The ITO targets were 91 molar % In<sub>2</sub>O<sub>3</sub> and 9 molar % SnO<sub>2</sub>. Earlier studies indicated that adding a small amount of H<sub>2</sub> to the Ar sputtering environment during ITO deposition substantially increased the open-

\* This work was supported by NASA Lewis Research Center under Interagency Order No.C-3000-K and by the U.S. Department of Energy under Contract No. DE-AC02-83CH10093.

circuit voltage ( $V_{oc}$ ) and fill factor (FF) of the resultant solar cell. [3] However, continued sputtering in this  $H_2$ -rich atmosphere progressively altered the target material, resulting in a poor control of the optical and electrical properties of the ITO. Thus, to provide greater compositional control of the ITO film(s), two US Guns have been incorporated into the vacuum system for this production. The first gun deposits ITO in an  $Ar/H_2$  atmosphere at a very slow deposition rate ( $\sim 0.01 \text{ nm sec}^{-1}$ ). Because the optical transmission of this  $H_2$ -rich ITO is poor, the thickness of this layer is limited to 5 nm. The remaining 50 nm of ITO is deposited with a second US Gun source. This layer reduces the emitter sheet resistance and completes the necessary thickness for the first layer of a two-layer ITO/ $MgF_2$  antireflection coating (ARC). For this second ITO deposition, an  $Ar/O_2/H_2$  ambient is used (" $O_2$ -rich" ITO); the  $O_2$  and  $H_2$  partial pressures are adjusted to yield optimum electrical and optical properties. Both the  $H_2$ -rich and the  $O_2$ -rich depositions are performed without breaking vacuum. Following deposition, ellipsometry and four-point probe measurement are used to determine the ITO thickness and sheet resistance, respectively. If the sheet resistance is found to be excessively high ( $1000\text{-}40,000 \text{ } \Omega/\square$ ), the ITO-coated cell is placed in a Technics Planar Etch II plasma etching system and exposed to a pure- $H_2$  plasma. This procedure reduces the sheet resistance of the ITO to  $\sim 600\text{-}800 \text{ } \Omega/\square$  while still maintaining optical clarity. It is believed that this process removes excess  $O_2$  for the ITO, thereby creating vacancy-generated carriers. (ref. 6)

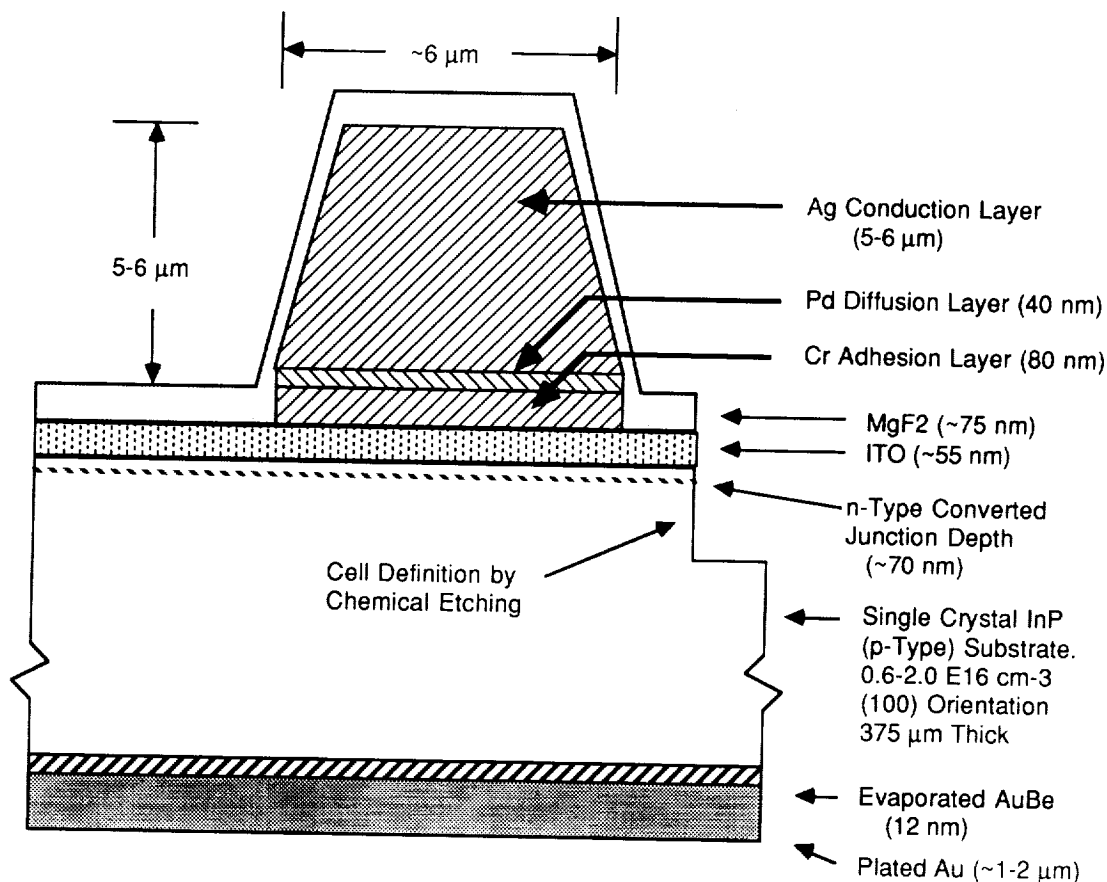


**Figure 1.** Cross-sectional view of ITO/InP solar cell showing metallization and antireflection coatings. Note high aspect ratio of grid line made possible by the photolithographic lift-off techniques used.

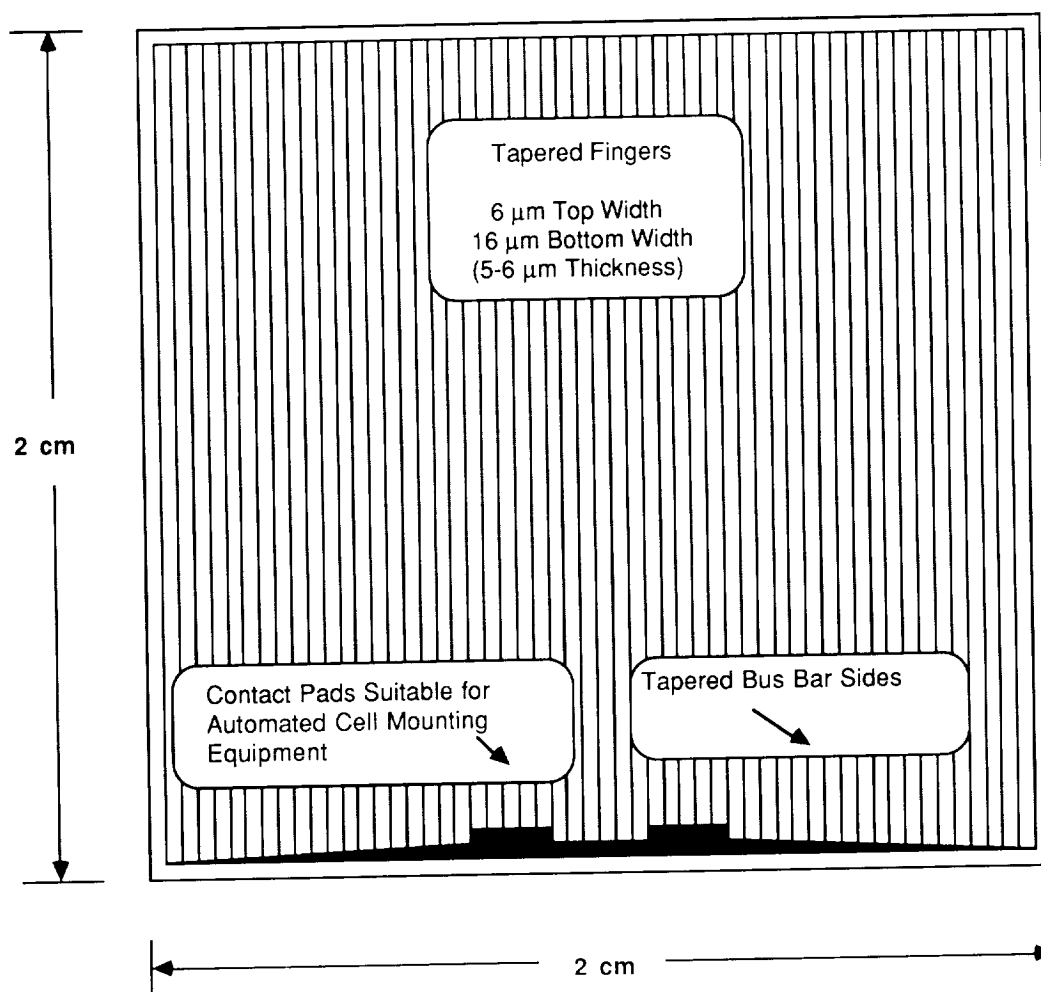


**Figure 2.** Plan view of grid design used on 4 cm<sup>2</sup> ITO/InP solar cells. The (modeled) losses of this grid are: Resistance ~2.8% and Shadowing ~3.3%, yielding a total grid losses ~6.1%.

After ITO deposition, top grid electrical contacts were patterned using an additive lift-off procedure involving chlorobenzene. (ref. 7 & 8) Following photolithography, but prior to metallization, the cells were plasma cleaned in Ar using the same Technics Planar Etch II system already mentioned. This promoted the adhesion of the the subsequent metallization. Metallization (See Figure 1) was performed in an electron-beam vacuum system with Cr/Pd/Ag layers of 80 nm, 40 nm, and 5 μm, respectively. (ref. 9) The top grid contact is an optimum design which, in addition to very high aspect-ratio grid lines, utilizes tapered bus bars and fingers (See Figure 2). The grid also included two relatively large contact pads and an interconnect between the pads, a design conforming to the requirements of semi-automatic mounting equipment currently used in the space industry. After metallization lift off, the active cell area was defined using photolithography and HCl chemical etching. Following cell definition, the second layer of the ARC was formed using resistively evaporated MgF<sub>2</sub>.

As a final process step before cell measurement, a post-deposition heat treatment (PDHT) at 125°C for 30 min was performed. This treatment increased the short-circuit current ( $J_{sc}$ ) of the cells by ~2% without adversely affecting other device parameters. This PDHT was necessary because the photolithographic processes used for this production are of lower temperature (<100°C) than those used in previous research (~120°C). Thus, PDHT occurs *automatically* if the photolithographic processing involves typically used temperatures. Although the PDHT does add an additional step to the process, it also yields the opportunity to isolate and study an aspect of the ITO/InP cell fabrication that has not been previously observed. After fabrication, the cells were characterized using quantum efficiency measurements and light and dark current-voltage measurements using standardized methods. (ref. 10)

## Results and Discussion

The project began with 38 1-in.<sup>2</sup> InP substrates of the low doping density range (low  $10^{16} \text{ cm}^{-3}$ ), and 20 substrates of the higher doping range (low  $10^{17} \text{ cm}^{-3}$ ). At this time, all of the  $10^{16} \text{ cm}^{-3}$  substrates have been fabricated into solar cells, but only one cell has been fabricated for the  $10^{17} \text{ cm}^{-3}$  material. Thus, most of the results presented here involve performance characteristics of cells made on the  $10^{16} \text{ cm}^{-3}$  material, although some preliminary, yet insightful results from the cell made on the higher-doped material will also be discussed. Of the 38 ( $10^{16} \text{ cm}^{-3}$ ) substrates, four were broken or damaged during back contacting procedures, one was broken during chemical etching, and one suffered grid adhesion loss. Shown in **Figure 3** and **Figure 4** is the range of demonstrated AM0 performance for the remaining 32 cells. From these data, the average cell efficiency is determined to be 15.5%, with a standard deviation of 0.35%. The highest cell performance obtained is 16.1% AM0 (SERI measurement). Dark I-V data analysis indicates that the cells demonstrate near-ideal characteristics, with a diode-ideality factor and reverse-saturation current density of 1.02 and  $1.1 \times 10^{-12} \text{ mAcm}^{-2}$ , respectively.

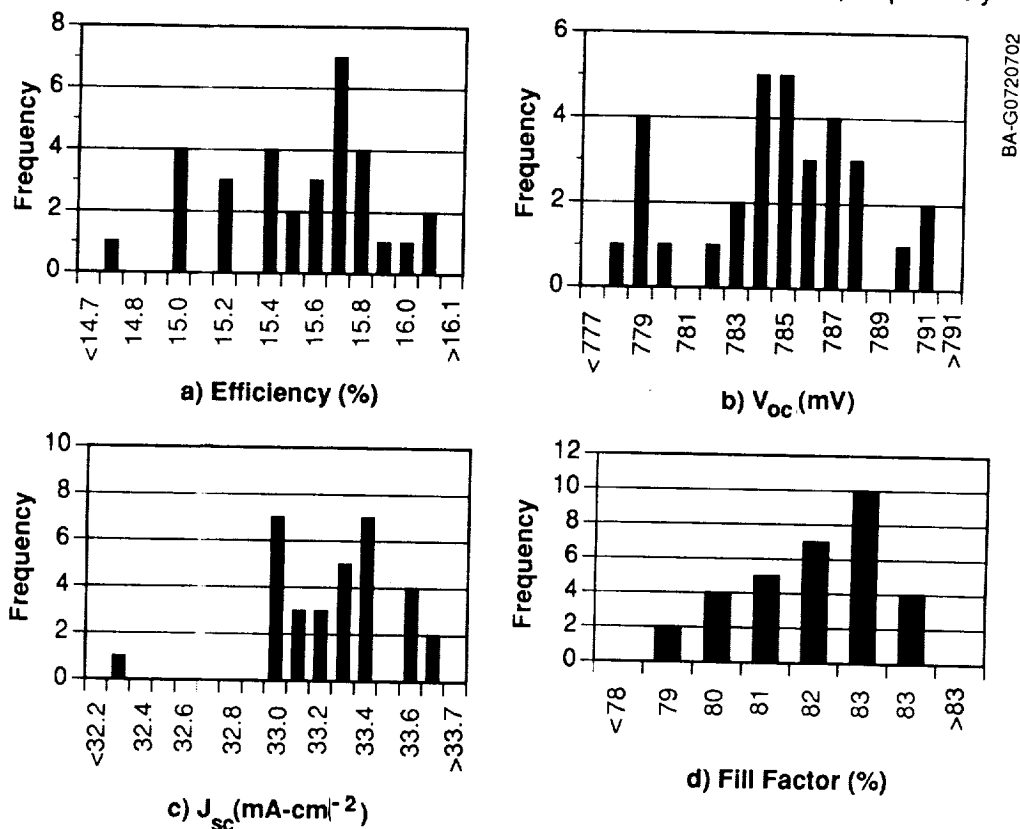
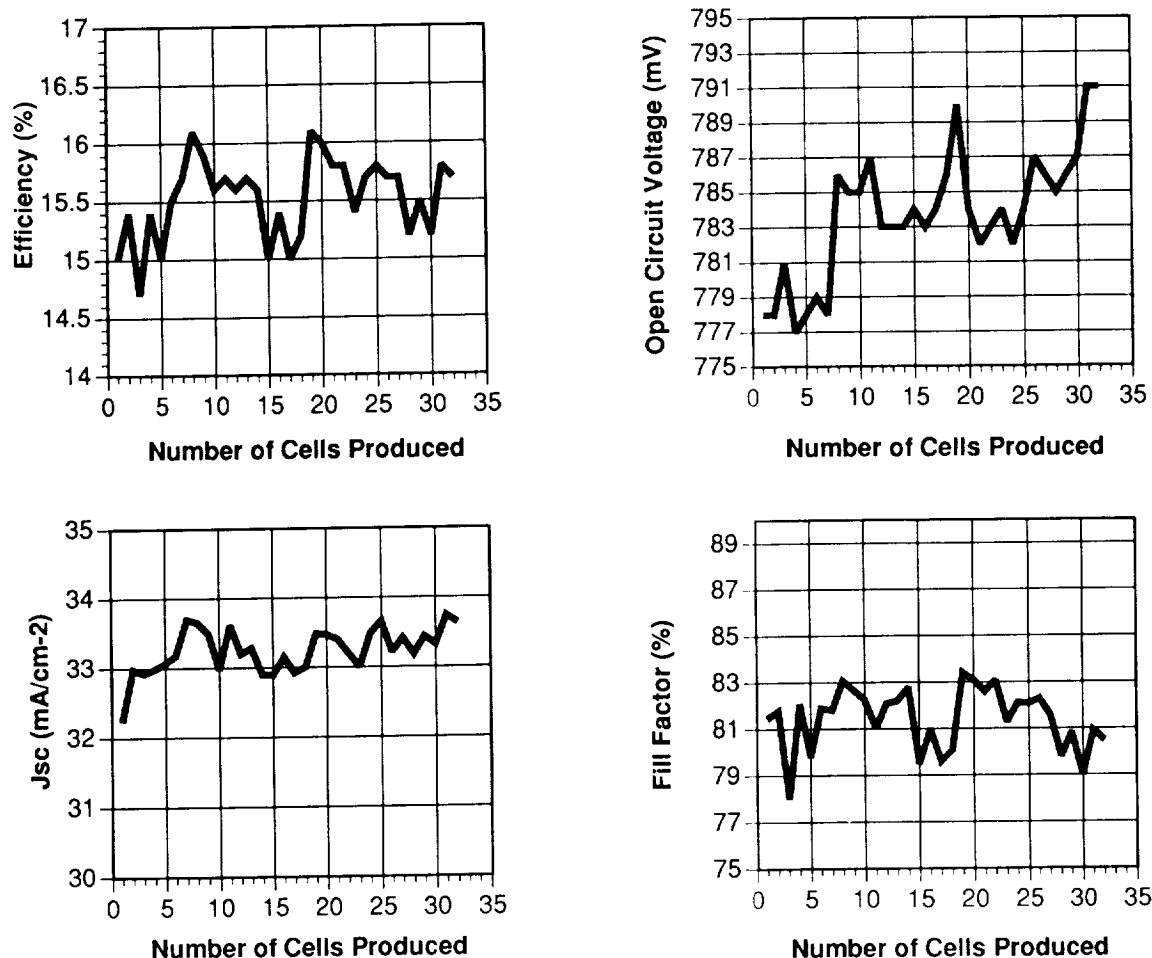


**Figure 3.** Histograms illustrating the AM0 ( $1367 \text{ Wm}^{-2}$ ) performance parameters of the 32  $4\text{-cm}^2$  ITO/InP solar cells fabricated during the small-scale production. a) Efficiency. b) Open-circuit voltage. c) Short-circuit current density. d) Fill factor.

As mentioned previously, the PDHT was found to increase the  $J_{sc}$  of the cells. However, as indicated by quantum efficiency analysis shown in **Figure 5**, the effect of the PDHT is not completely beneficial. Indeed, although during PDHT the central and short-wavelength response is enhanced, the long-wavelength response is noticeably reduced. A plausible explanation for this is that the PDHT tends to reduce the extent of type-conversion throughout the junction region, with the overall effect being to shift the effective depth of the sputter-formed junction nearer the surface. This is consistent with earlier observations, in which higher-temperature heat treatments ( $200^\circ\text{C}$ ) resulted not only in increased current density but severely reduced  $V_{oc}$ . (ref. 11) However, in this earlier work, a reduction in the long-wavelength QE was not observed, probably because the substrates and processes used at that time resulted in much poorer long-wavelength response.



BA-G0720701

**Figure 4.** AM0 performance characteristics of the 32 4-cm<sup>2</sup> ITO/InP solar cells as a function of fabrication experience. Note that the only performance parameter that indicates a slight progressive improvement is the  $V_{OC}$ .

Shown in **Figure 6** is the light current-voltage characteristics of one of the two best 4-cm<sup>2</sup> cells made on the  $10^{16}$  cm<sup>-3</sup> material, demonstrating an AM0 efficiency of 16.1% (SERI measurement). By comparing these data with those taken from the best small-area cell produced (16.5% AM0, 0.1 cm<sup>2</sup>, SERI measurement), (ref. 3) one notes that the  $J_{SC}$  and the FF values are nearly identical. This not only suggests that the junction-formation mechanism is spatially very uniform, but also that the grid design/metallization are nearly optimal for this 4-cm<sup>2</sup> cell. Only  $V_{OC}$  is lower (by ~10-20 mV) than that previously measured on best smaller ITO/InP cells made from previously used bulk material. At present, the reason for this is not apparent. Past observations from these ITO/InP cells have indicated a trend of decreasing  $V_{OC}$  with increasing substrate doping (i.e., increasing  $N_A$ ). (ref. 3 & 12) However, the recent results from the cell fabricated on the  $10^{17}$  cm<sup>-3</sup> substrate, as discussed below, indicate that the substrates and processes used for this production demonstrate the opposite (but more classical) behavior of increasing  $V_{OC}$  with increasing substrate doping.

Although the efficiency spread of the cells made on the  $10^{16}$  cm<sup>-3</sup> substrates is quite small, it should be noted that several process-related aspects strongly affected the measured performance of the individual cells. Perhaps the most important of these is the amount of time during which the cell is exposed to air between ITO and MgF<sub>2</sub> deposition. Indeed, a cell will degrade by up to ~5 mV per week if it is not capped with MgF<sub>2</sub>. A possible explanation for this is that the sputtered ITO is believed to be relatively porous, allowing O<sub>2</sub> diffusion and subsequent reaction at the emitter/ITO interface. Here, the O<sub>2</sub> may neutralize the passivating effect of the H<sub>2</sub>. The evaporated MgF<sub>2</sub>, however, may be much less porous, reducing O<sub>2</sub> diffusion. Other parameters that were initially difficult to control were the sheet resistance, transparency, and thickness of the ITO. As observed in earlier work, care must be taken to maintain an optimum combination of electrical and optical properties of the ITO as the sputtering source erodes.

Although this can be accomplished through small adjustments in the O<sub>2</sub>/H<sub>2</sub> ratio of the sputtering ambient of the O<sub>2</sub>-rich ITO layer, considerable variation is still observed. Luckily, the effects of this problem (FF reduction) were virtually eliminated once the post-deposition H<sub>2</sub> plasma exposure procedure was developed and implemented. The final area of noted weakness in device fabrication was the back contacting procedure. It was during this part of cell production that the majority of cell breakage occurred. The underlying reason for this appears to be that, although the two-step back metallization procedure gives a reliably low-resistance ohmic contact, it involves many steps in which the substrate is physically handled (e.g., during wax mounting, chemical etching, annealing, etc.). Because most of this handling results from the requirement to remove the BeO that forms during sintering, (ref. 5) it has been suggested that other contacting procedures could be developed that would make use of either different metals and/or entirely in-vacuo process techniques.

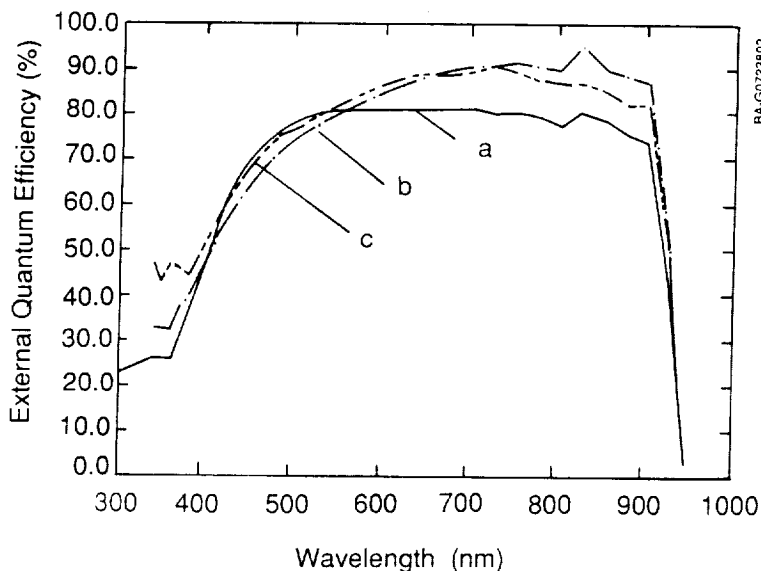


**Figure 5.** External quantum efficiency of a 4-cm<sup>2</sup> ITO/InP cell produced on 10<sup>16</sup> cm<sup>-3</sup> substrate material. a) ITO only. b) ITO/MgF<sub>2</sub>. c) ITO/MgF<sub>2</sub> after post-deposition heat treatment.

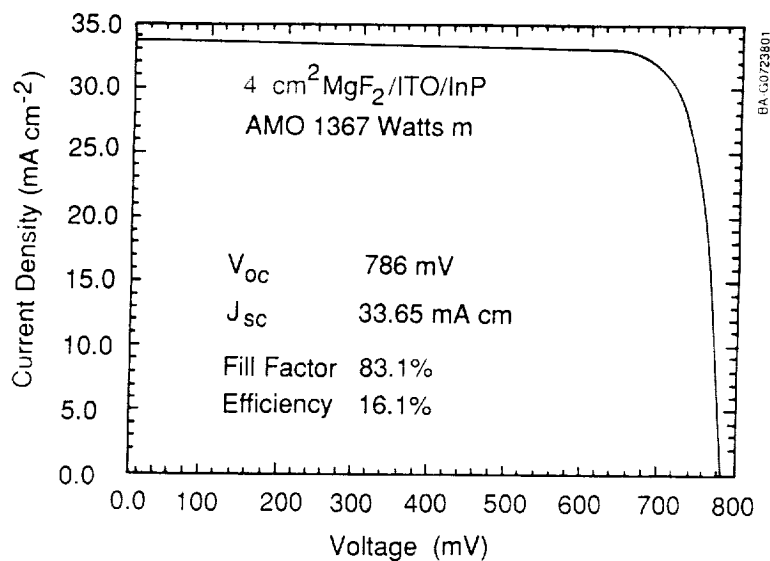


**Figure 6.** Light I-V characteristics of one of the best 4-cm<sup>2</sup> ITO/InP cell produced from 10<sup>16</sup> cm<sup>-3</sup> substrate material.

As mentioned previously, 20 substrates with a higher doping density of  $1-2 \times 10^{17} \text{ cm}^{-3}$  were supplied by AT&T Microelectronics. Because earlier research had indicated that the best cell performance has always been achieved on  $10^{16} \text{ cm}^{-3}$  material, only a single device has thus far been fabricated on the  $10^{17} \text{ cm}^{-3}$  material. Although it was thought that the performance of this device would, as in the past, be much poorer than that of the  $10^{16} \text{ cm}^{-3}$  material (due to reduced  $V_{oc}$  and  $J_{sc}$ ), **Figure 7** shows the surprising result that an efficiency of 15.8% AM0 (SERI measurement) was achieved. Perhaps the most noteworthy feature of this result is that, instead of a reduced  $V_{oc}$ , as was always observed in past research, the  $V_{oc}$  is 12 mV higher than that from the best of the 32 cells made from the  $10^{16} \text{ cm}^{-3}$  material (nearly 20 mV greater than the average  $V_{oc}$  measured for the 32 cells). However, because the long-wavelength portion of the QE is reduced, the  $J_{sc}$  of this cell is ~3% lower than that of cells made on the  $10^{16} \text{ cm}^{-3}$  material. Presently, studies are ongoing to determine if the grid design can be modified to function without the benefits of the ITO (lower sheet and contact resistance). If this can be done, better optical matching of the ARC may be possible. For example, if a material such as ZnS replaces the ITO, modeling studies indicate that the  $J_{sc}$  of these ( $10^{17} \text{ cm}^{-3}$ ) cells would increase to ~33.8  $\text{mAcm}^{-2}$ . If this can be done while maintaining current values of FF and  $V_{oc}$ , then the efficiency would increase from 15.8% to 16.3% AM0. In addition, because the ZnS is less absorbing than the ITO, modeling results also suggest that  $J_{sc}$  values up to 36.5  $\text{mAcm}^{-2}$  may be possible (assuming 4% shadow loss); this would result in a cell with an efficiency of ~17.7% AM0. Finally, because these large-area cell results indicate that the junction formation is relatively insensitive to surface irregularities, investigations are ongoing in collaboration with researchers at NASA Lewis Research Center to determine what effects deliberate surface texturing (V-Groove) may have on the junction parameters (ref. 13). If these parameters are insensitive to texturing, further increases in current collection may be possible.

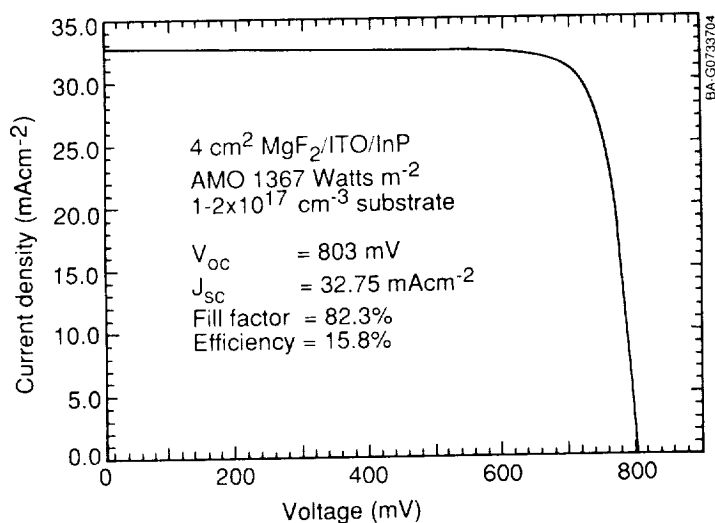


**Figure 7.** Light I-V characteristics of a 4-cm<sup>2</sup> ITO/InP cell produced from  $10^{17} \text{ cm}^{-3}$  substrate material. Note that the  $V_{oc}$  is higher than for the  $10^{16} \text{ cm}^{-3}$  material but that the  $J_{sc}$  is slightly reduced.

## Conclusions

This project has demonstrated that the sputtering process used to form small-area ITO/InP solar cells can readily be scaled to produce large-area ( $4\text{-cm}^2$ ) devices. These large-area cells demonstrate nearly identical performance to similar small-area cells, suggesting that the spatial independence of the junction-formation mechanism may be exploited further to productions involving larger batches. These results also suggest that this method of junction fabrication is not as sensitive to the same predeposition surface irregularities, which tend to have devastating effects in other solar cell technologies. The highest resultant solar cell efficiency from the 32 cells produced on substrate material doped  $0.5\text{-}2.0 \times 10^{16} \text{ cm}^{-3}$  is 16.1% AM0 (SERI measurement), which is comparable to the highest efficiency reported from another *production* method using closed-ampoule diffusion. Additionally, because the sputter-deposition technology can be configured for in-line (rather than only batch) production modes, this process may possess additional economic advantages. Finally, since the substrates used for this production were acquired from a US supplier, this technique represents a completely US-based technology for manufacturing radiation-hard solar cells.

## References

1. Weinberg, I., C.K. Swartz, R.E. Hart, Jr., and T.J. Coutts. 1988. Radiation Resistance and Comparative Performance of ITO/InP and N/P InP Homojunction Solar Cells. Proc. 20th IEEE Photovoltaic Specialists Conf., Las Vegas, NV. Sept. 26-30 (IEEE, New York, 1988) 893-897.
2. Yamaguchi, M., T. Hayashi, A. Ushirokawa, Y. Takahashi, M. Koubata, M. Hashimoto, H. Okazaki, T. Takamoto, M. Ura, M. Ohmori, S. Ikegami, H. Arai, and T. Orii. First Flight of InP Solar Cells. 1990. Proc. 21st IEEE Photovoltaic Specialists Conf., Kissimmee, FL, May 21-25 (IEEE, New York, 1990) 1198-1202.
3. Gessert, T.A., X. Li, M.W. Wanlass, A.J. Nelson, and T.J. Coutts. Investigation of Buried Homojunctions in p-InP Formed During Sputter Deposition of Both Indium Tin Oxide and Indium Oxide. 1990. J. Vac. Sci. Technol. A, **8** (3) 1912-1916.
4. Gessert, T.A., X. Li, M.W. Wanlass, and T.J. Coutts. 1990. Progress in the ITO/InP Solar Cell. Proc. Second Int. Conf. on InP and Related Mat., Denver, CO. April 23-25, 1990, IEEE Cat. No. 90CH2895 (IEEE, New York, 1990) 260-264.
5. Gessert, T.A., X. Li, T.J. Coutts, M.W. Wanlass, and A.B. Franz. 1989. Aspects of Processing Indium Tin Oxide/InP Solar Cells. Proc. First Int. Conf. on Indium Phosphide and Related Mat. for Adv. Electronic and Optical Devices, Norman, OK, March 20-22, 1989, SPIE Proceedings Vol. 1144 (SPIE, Bellingham, WA, 1989) 476-487.
6. Gessert, T.A., D.L. Williamson, T.J. Coutts, A.J. Nelson, K.M. Jones, R.G. Dhere, H. Aharoni, and P. Zurcher. 1987. The Dependence of the Electrical Properties of Ion-Beam Sputtered Indium Tin Oxide on its Composition and Structure. J. Vac. Sci. Technol. A, **5** (4) 1314-1315.
7. Gessert, T.A., X. Li, and T.J. Coutts, presented at the 10th PVAR&D Meeting, Lakewood, CO, Oct. 23-25, 1990, to be published in Solar Cells.
8. Hatzakis, M., B.J. Canavello, and J.M. Shaw. 1980. Single-Step Optical Lift-Off Process. IBM J. Res. Develop., **24** (4) 452-460.
9. Gessert, T.A., and T.J. Coutts. 1990. Requirements of Electrical Contacts to Photovoltaic Solar Cells. MRS Proc. Vol. 181 (MRS, Pittsburgh, PA, 1990) 301-312.
10. "Standard Test Methods for Electrical Performance of Non-Concentrator Photovoltaic Cells Using Reference Cells," ASTM Standard E948.
11. Coutts, T.J., X. Wu, T. A. Gessert, and X. Li. 1988. Direct-Current Magnetron Fabrication of Indium Tin Oxide/InP Solar Cells. J. Vac. Sci. Technol. A, **6** (3) 1722-1726.
12. Coutts, T.J., and S. Naseem. 1985. High Efficiency Indium Tin Oxide/Indium Phosphide Solar Cells. Appl. Phys. Lett., **46** (2) 164-166.
13. Bailey, S., N. Fatemi, G.A. Landis, D. Brinker, M. Faur, and M. Faur. 1990. Application of V-Groove Technology to InP Solar Cells. Proc. Second Int. Conf. on InP and Related Mat., Denver, CO. April 23-25, 1990, IEEE Cat. No. 90CH2895 (IEEE, New York, 1990) 73-79.